

Machine Learning for Extrapolating No-Core Shell Model Results to Infinite Basis

R. E. Sharypov^a, A. I. Mazur^a, A. M. Shirokov^b

^a*Pacific National University, 136 Tihookeanskaya street, Khabarovsk, 680035, Russia*

^b*Skobeltsyn Institute of Nuclear Physics, Lomonosov Moscow State University, Leninskie Gory 1/2, Moscow, 119991, Russia*

Abstract

We utilize the machine learning to extrapolate to the infinite model space the no-core shell model (NCSM) results for the energies and rms radii of the ${}^6\text{He}$ ground state and ${}^6\text{Li}$ lowest states. The extrapolated energies and rms radii converge as the NCSM results from larger model spaces are included in the training dataset for ensemble of artificial neural networks thus enabling an accurate predictions for these observables.

Keywords: No-core shell model, *ab initio* approaches, machine learning, artificial neural networks, extrapolation of variational calculations

1. Introduction

Machine learning methods are increasingly utilized in both theoretical and experimental studies of atomic nuclei [1]. In this paper, we continue exploring the machine learning techniques for extrapolating results of variational calculations of nuclear observables to infinite model spaces.

The no-core shell model (NCSM) [2] is currently one of the most promising *ab initio* approaches to theoretical investigations of nuclei. In the NCSM, all nucleons are spectroscopically active, and their motion is governed exclusively by the chosen model of realistic nucleon-nucleon (NN) and, if needed, three-nucleon ($3N$) interactions, without any phenomenological assumption.

Email addresses: 2017104939@togudv.ru (R. E. Sharypov),
amazur.pnu.khb@mail.ru (A. I. Mazur), shirokov@nucl-th.sinp.msu.ru
(A. M. Shirokov)

The NCSM basis states are constructed as Slater determinants of single-particle harmonic oscillator wave functions. The NCSM parameters are the oscillator energy $\hbar\Omega$ and the size of the model space, characterized by the maximum number of excitation quanta N_{\max} allowed for in the calculation. The NCSM basis functions for a nucleus with A nucleons include all possible combinations of nucleons with total oscillator quanta ranging from N_{\min} to $N_{\min} + N_{\max}$, where N_{\min} is the minimal oscillator quanta allowed for the nucleus as dictated by the Pauli exclusion principle.

The NCSM results are exact in the limit $N_{\max} \rightarrow \infty$. However, the dimensionality of the many-body basis grows exponentially with increasing N_{\max} , which restricts calculations with a reasonable precision, even on modern supercomputers, to light nuclei with mass numbers $A \lesssim 20$. Therefore, developing robust methods for extrapolating results to infinitely large model spaces remains a pressing challenge.

Most extrapolation methods developed to date [3, 4, 5, 6, 7, 8, 9, 10] lack rigorous theoretical justification limiting their applicability. The most theoretically grounded approach [10] involves localizing the poles of the S -matrix for bound states.

Machine learning offers a promising alternative for addressing this problem. This direction is also of independent interest as an application of the machine learning to extrapolation problems requires the development of novel algorithms and theoretical approaches, opening new avenues for research.

The first study of the machine learning extrapolation of variational calculation results to the infinite model space was presented in Ref. [11]. The extrapolation method of Ref. [11] (ISU) involves training an ensemble of artificial neural networks to predict the target observable (e. g., energy E , rms point-proton radius r_p , etc.) based on a set of calculations of a nucleus of interest performed within the NCSM. Each neural network is a single-layer perceptron. The inputs are the NCSM parameters, N_{\max} and $\hbar\Omega$, while the outputs are the NCSM results for the observable of interest obtained with these input parameters. The trained neural networks are used to predict the results at very large values of N_{\max} where the convergence of the NCSM calculations is supposed to be achieved. Later a similar approach was employed for the NCSM result extrapolations in Refs. [12, 13].

There is an alternative machine learning approach TUDa to the extrapolation of NCSM calculations developed in Refs. [14, 15]. Instead of training neural networks for each particular nucleus, TUDa suggests an universal neural network ensemble trained on NCSM results for light nuclei where a

complete convergence is achievable, using various NN interactions. This universal ensemble is used for extrapolating the NCSM results for heavier p -shell nuclei. A benchmarking of ISU and TUDa methods for the ground state energies and point-proton radii of Li isotopes [16] demonstrated the consistency of the obtained results within the estimated uncertainties.

In this study, we continue the neural network extrapolation studies following the route suggested in the pioneering Ref. [11] with modifications discussed below which we suggested in Refs. [17, 18]. We present the extrapolated results for the ground state energies of the ${}^6\text{He}$ and ${}^6\text{Li}$ nuclei and for the lowest excited state energies of ${}^6\text{Li}$ as well as for the rms point-proton r_p , point-neutron r_n , and point-nucleon (matter) r_m radii in these states, based on NCSM calculations conducted in model spaces with $N_{\text{max}} \leq 18$ using the realistic NN interaction Daejeon16 [19].

The manuscript is organized as follows. A description of the method employed is presented in Section 2. The results of extrapolations of the considered observables in ${}^6\text{He}$ and ${}^6\text{Li}$ are presented and discussed in Section 3. Finally, a short summary and the conclusions are given in Section 4.

2. Method

The outline of our method is that we employ an ensemble of randomly initialized artificial neural networks to analyze results of the NCSM calculations and predict observables at very large N_{max} values where the convergence of the NCSM calculations is supposed to be achieved. The ensemble approach aims to improve the prediction accuracy and to assess its uncertainty.

As compared with the pioneering work [11], we proposed a different neural network topology and established strict criteria for selecting trained neural networks [17, 18]. This eliminates the need to split the data into training and testing sets, significantly simplifying the training process [17]. Our modified approach, combined with rigorous statistical analysis of predictions from the selected networks, ensures statistical robustness and increases the reliability of the extrapolated results.

The proposed extrapolation method was tested on a benchmark problem of calculations of the deuteron ground state energy supported by the realistic Nijmegen II NN potential [20]. This problem exhibits a slow convergence with different behaviors of the results obtained with odd and even values of $N_{\text{max}}/2$ thus posing additional challenges for extrapolation techniques, and provides a unique opportunity to verify the correctness and efficacy of

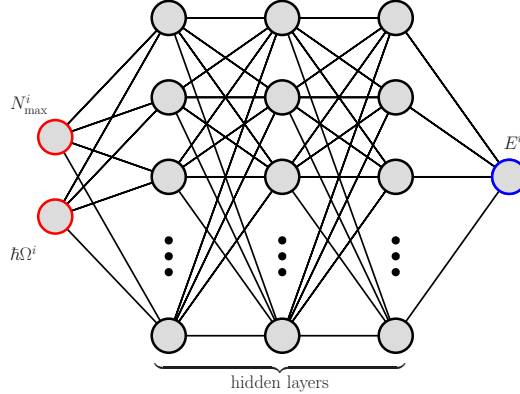


Figure 1: Neural network architecture

the developed algorithm. We note also that the dependence on the oscillator frequency $\hbar\Omega$ of the deuteron energy obtained with the Nijmegen II, demonstrates a complex behavior characterized by the formation of two local minima, making it particularly conclusive for testing machine learning extrapolation capabilities.

2.1. Neural network design

Network architecture. The proposed model consists of an ensemble of 1024 fully connected feedforward neural networks, each designed to handle the structured NCSM data. Each neural network is multilayer perceptron with identical architectures comprising an input layer, three hidden layers, and an output layer as shown in Fig. 1. The input layer consists of 2 neurons. One of the input layer neurons receives the N_{\max} value, another receives the $\hbar\Omega$ value; these values are transmitted to the neurons of the first hidden layer. Each neuron i of hidden layers collects the signals y_j^i from all neurons of the previous layer, sums them with its individual set of weights w_j^i , adds a bias b^i to obtain $x^i = \sum_j w_j^i y_j^i + b^i$ and uses the activation function $f(x)$ to obtain the signal $f(x^i)$ which is transmitted to all neurons of the next layer. The output layer does the same to produce the result $f(x^i)$ of the calculation performed by the artificial neuron network. The weights w_j^i and biases b^i constitute a set of trainable network parameters.

The first hidden layer contains 10 neurons and employs the identity activation function $f(x) = x$. The second and the third hidden layers each contain 10 neurons and utilize the sigmoid activation function $f(x) = 1/(1 + \exp(-x))$.

The output layer consists of a single neuron with the identity activation function. The random initialization of weights and biases follows the default Glorot initialization method [21]. The machine learning model is implemented using Keras [22] with TensorFlow [23] as the backend. Programming code is available on GitHub [24].

The chosen neural network architecture, particularly the use of the sigmoid activation function, leads to the saturation when large N_{\max} values are provided as the input. As a result, in the limit $N_{\max} \rightarrow \infty$, the neural network predictions become independent of $\hbar\Omega$.

The use of the linear activation function in the output layer allows to generate predictions over a wide range of $\hbar\Omega$ without being constrained by the limiting values of the activation function; the saturation at large N_{\max} occurs in the network hidden layers.

Data and Preprocessing. The neural network input includes the NCSM parameters N_{\max} and $\hbar\Omega$, while the output corresponds to the calculated observables (e. g., energy of a given state E , rms point-proton r_p , point-neutron r_n or point-nucleon r_m radii). The dataset composed of N_{\max} , $\hbar\Omega$, E (or r_p , or r_n , or r_m) serves as the training set. It was shown in Ref. [10] that stable extrapolation results for energies using the SS-HORSE–NCSM method are only achieved if, in each model space, the data lying to the right of the variational minimum in $\hbar\Omega$ are considered. Based on our experience gained in numerical calculations, we conclude that this selection of data also significantly improves extrapolations utilizing machine learning. The right cutoff value of $\hbar\Omega = 40$ MeV is applied both for radii and energies while the left cutoff value for radii we set to $\hbar\Omega = 12.5$ MeV. We use for the training the NCSM results obtained with a set of different $\hbar\Omega$ values in the model spaces $N_{\max} = 4, N_{\max} = 6, \dots, N_{\max} = N_{\max}^u$ and increase N_{\max}^u to examine the convergence of the obtained predictions. Prior to training, the data of each type in the training set is normalized to a standard range of $[0, 1]$.

Training process. Each network is trained using the Adam optimization algorithm [25], which provides internal adaptive learning rates and efficient gradient-based optimization. Additionally, an external triangular cyclical learning rate schedule [26] is employed to dynamically adjust the learning rate during training, improving convergence. This schedule is implemented with TensorFlow Addons [27] library. The learning rate cycles between the base value of 10^{-4} and the amplitude value which is equal to 10^{-2} at the

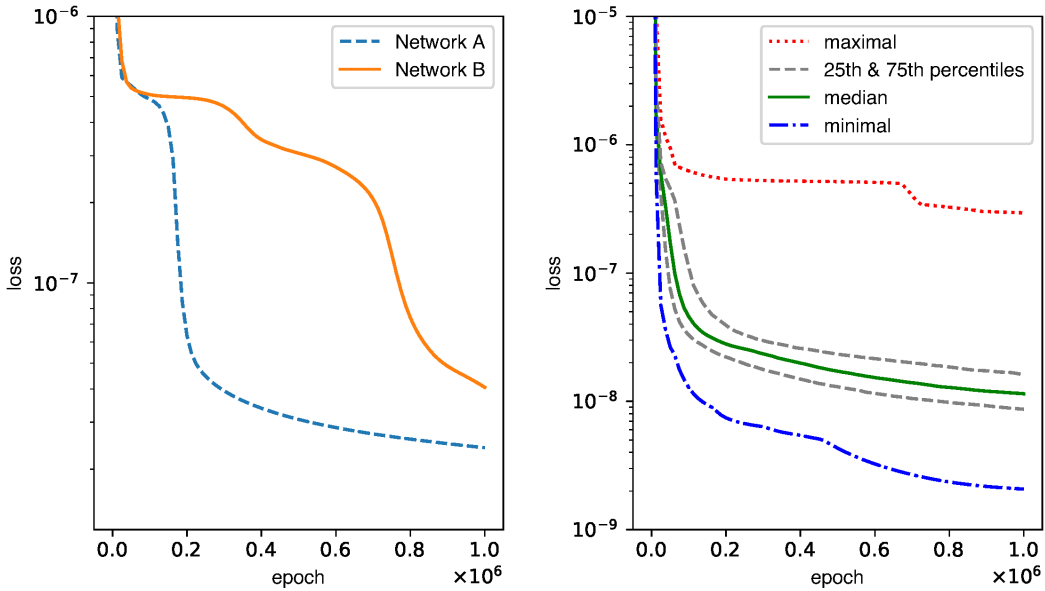


Figure 2: Evolutions of loss functions during training on the ${}^6\text{Li}$ ground state energy datasets with $N_{\text{max}}^u = 18$. Left panel: evolutions of two different networks during the training; right panel: median loss function of the network ensemble (green solid curve), minimal (blue dash-dotted curve) and maximal (red dotted curve) loss function values, 25th and 75th percentiles of the loss distribution (gray dashed curves).

beginning of the training and decreases during the training. This forms a decaying sawtooth pattern of the learning rate with large values providing a rough convergence and smaller values providing the fine tuning of the neural network.

The batch size is fixed at the length of training set to balance computational efficiency and convergence speed. The loss function is defined as the mean-square deviation ensuring minimization of the discrepancy between predicted and actual values. The training process is conducted over 10^6 epochs. Additional details of the training can be found in Refs. [17, 18].

Training each neural network for 10^6 epochs may seem excessive; however, even over such an extended period, the loss function exhibits rapid changes within a small number of optimization steps occurring unpredictably at any stage, as illustrated in Fig. 2 (left panel) where we present evolutions of two different networks during the training on the same datasets with $N_{\text{max}}^u = 18$. Moreover, the right panel of Fig. 2 demonstrates that the ensemble as a whole continues to improve with the median loss function value (green solid

curve) steadily decreasing throughout the training process. The blue dash-dotted and red dotted curves represent the minimal and the maximal loss function values, respectively, while the gray dashed curves are the plots of the 25th and 75th percentiles of the loss distribution. The loss function values presented in Fig. 2 were taken only at the end of each training cycle. These observations suggest that an early stopping may not be an optimal strategy in this problem.

This behavior may be attributed to the cyclical learning rate schedule. This behavior may be related also to the phenomenon of grokking [28], where an ensemble with the increasing number of neural networks undergoes a phase transition, shifting to significantly lower loss values. As a result, while individual networks may experience abrupt improvements, the ensemble as a whole exhibits a relatively smooth and continuous learning trajectory. However, an additional research is required to explicitly demonstrate the effect of grokking.

The set of hyperparameters outlined in this section (but not limited to) controlling the machine learning process has been designed and carefully tested in the described above benchmark problem of extrapolating the ground state energy of the ^2H nucleus supported by the Nijmegen II NN potential.

2.2. Prediction processing

Not all trained neural networks produce reasonable predictions, thus it is needed to establish selection criteria for networks in the ensemble. The selection process consists of three main stages [17, 18]: constructing a prediction array including results from different model spaces, applying filtering criteria to retain only reliable networks, and filtering the outliers.

Prediction array construction. The prediction array is obtained by generating the results for model spaces $N_{\max}^u + 2, N_{\max}^u + 4, \dots, N_{\max}^f$ and the range of $\hbar\Omega$ values matching that of the training dataset. We use $N_{\max}^f = 300$ as the upper limit for the model space predictions.

Selection criteria. To ensure the reliability and stability of the ensemble, we apply the following selection criteria:

- “Soft” Variational Principle (for energies only): The predictions obtained with increasing N_{\max} at the same $\hbar\Omega$ values may exhibit minor violations of the variational principle due to numerical errors which are not exceeding 0.1 keV.

- $\hbar\Omega$ Independence (or weak dependence): At $N_{\max}^f = 300$, the predictions should be stable with respect to the $\hbar\Omega$ variations. We impose the maximal allowable deviations of 2 keV for energies and of 0.002 fm for radii.
 - Convergence Principle (for energies only): For each network in the ensemble, a critical model space N_{\max}^c is defined such that the network predictions for this model space fit the following two conditions. (1) In the model space $N_{\max} = N_{\max}^c$, the difference between the predicted maximal and minimal energies in the range of $\hbar\Omega$ values included in the prediction array do not exceed 20 keV. (2) The difference between the predicted minimal energy values in adjacent model spaces $N_{\max} = N_{\max}^c$ and $N_{\max} = N_{\max}^c + 2$ do not exceed 1 keV.
- From the networks that meet these criteria, the 20% with the highest N_{\max}^c values are discarded to ensure fast enough convergence behavior.
- Loss-Based Filtering: The 5% of networks with the largest loss function values at the end of training are also discarded.

Outlier Filtering. Following the above initial selection procedure, an additional outlier filtering step is performed [18]. For each neural network, predictions at $N_{\max} = N_{\max}^f$ are taken. In the case of energy predictions, the minimal value is determined for the range of $\hbar\Omega$ values. For the radius predictions, the arithmetic mean is calculated for the range of $\hbar\Omega$.

This yields a distribution of extrapolated energy or radius values in the network ensemble. To remove outliers from this distribution, we apply the boxplot rule as described in Ref. [29].

A neural network is excluded from further statistical analysis if it fails to meet any of the above selection criteria. This ensures that only models exhibiting stable and physically consistent predictions contribute to the final ensemble results, enhancing the reliability of the overall approach.

Final Estimation and Uncertainty Quantification. For the filtered prediction array at N_{\max}^f , the median value is computed and serves as the final estimate of the observable. The interquartile range between the 25th and 75th percentiles is used as a measure of the extrapolation uncertainty.

Nucleus (state)	Var. min.	Extrap. B	This work	Other	Experim.
${}^6\text{He}$ (g. s.)	-29.377	-29.41(1)	$-29.429^{+0.007}_{-0.005}$	-	-29.269
${}^6\text{Li}$ (g. s.)	-31.977	-32.007(9)	-32.036(3)	-32.061(4) ISU-a -32.036(20) ISU-b -32.011 $^{+0.006}_{-0.014}$ TUDa	-31.995
${}^6\text{Li}$ ($3^+,0$)	-30.072	-30.102(12)	$-30.129^{+0.004}_{-0.003}$	-	-29.809
${}^6\text{Li}$ ($0^+,1$)	-28.481	-28.507(4)	$-28.552^{+0.008}_{-0.005}$	-	-28.434

Table 1: Extrapolation results for the energies (in MeV) of the ${}^6\text{He}$ and ${}^6\text{Li}$ ground states and the lowest excited states in ${}^6\text{Li}$ obtained using the largest training dataset ($N_{max}^u = 18$) in comparison with the variational minimum obtained in the NCSM calculations at $N_{max} = 18$, with phenomenological extrapolation B [4], with machine learning approaches ISU-a of Ref. [11] and ISU-b [16] utilizing a smaller range of $\hbar\Omega$ values for training, with extrapolation TUDa using universal ensemble of neural networks [16], and with experiment [30]. The symmetric uncertainties of the last presented digits are given in parentheses while asymmetric uncertainties are given in super and subscripts.

3. Results

The ${}^6\text{Li}$ nucleus is of particular interest since its ground state energy and rms point-proton radius r_p have been studied using the machine learning extrapolation in the pioneering work [11]. Moreover, the training datasets obtained in the NCSM calculations with the Daejeon16 NN interaction were utilized in our study and in Ref. [11] as well as in a recent investigation of Ref. [16] which benchmarks two different approaches to the neural network training, one is the approach of Ref. [11] and the other is the approach developed in Refs. [14, 15]. There are key differences between these approaches: Ref. [11] suggests training an ensemble of artificial neural networks for each observable in each particular nucleus while the Refs. [14, 15] suggest an ensemble of universal networks for a set of nuclei trained on a particular observable in lightest nuclei. The approach of Ref. [11] is close to ours, however, there are essential differences including the neural network topology, selection criteria for trained networks, and several other methodological aspects.

The extrapolated energy values for the ${}^6\text{He}$ ground state and a few lowest states in ${}^6\text{Li}$, along with their associated uncertainties, are summarized in Table 1. For comparison, we present in Table 1 the results obtained by the phenomenological exponential extrapolation B [4], by the machine learning extrapolation approach of Ref. [11] (ISU-a), by the same approach utiliz-

ing a smaller range of $\hbar\Omega$ values for the network training (ISU-b) [16], by the approach of Refs. [14, 15] utilizing the ensemble of universal networks (TUDa) [16], as well as the respective experimental data [30] and variational minima in the NCSM calculations at $N_{\max} = 18$, i.e., in the largest model space used for the training of neural networks. Our energy predictions lie below those obtained by the extrapolation B clearly demonstrating inaccuracy of this phenomenological approach.

Our previous studies [17, 18] showed that a proper selection of the training dataset is essential for obtaining reliable predictions of extrapolated observables. For the energy extrapolations, we limited the training dataset to the $\hbar\Omega$ values ranging from the variational minimum for each model space up to 40 MeV. The ISU-a predictions were obtained based on the NCSM data spanning the $\hbar\Omega$ range from 8 to 50 MeV while the ISU-b results were obtained with the same neural network model trained on the data from the $\hbar\Omega$ range from 10 to 30 MeV. As seen in Table 1, the choice of the training dataset significantly impacts both the convergence behavior and the final predictions for the energies. In the case of the ${}^6\text{Li}$ ground state, our extrapolated energy lies above the ISU-a result and is consistent with the ISU-b estimation which, however, is characterized by a much larger uncertainty. Notably, the estimated ISU-a uncertainty interval does not overlap with those obtained by other machine learning approaches indicating that that one should be very accurate in applications of these approaches to extrapolating nuclear observables. It is important to emphasize that our approach employing a larger ensemble of trained neural networks and strict selection criteria, yields predictions with higher statistical reliability and weaker dependence on N_{\max}^u .

For the rms radii extrapolations, as follows from our studies in Refs. [17, 18], the optimal training datasets include the NCSM results obtained with $\hbar\Omega$ values ranging from 12.5 to 40 MeV. The convergences of the extrapolated rms point-proton, point-neutron, and point-nucleon (matter) radii of the ${}^6\text{Li}$ ground state as N_{\max}^u increases, are presented in Fig. 3. The final results obtained using the largest training dataset which includes all NCSM results from calculations in the model spaces $N_{\max} \leq N_{\max}^u = 18$, can be found in Table 2. Our predictions exceed both experimental values and the phenomenological $2D$ twisted tape extrapolation (TTE) results [32] based also on the NCSM calculations with Daejeon16.

The importance of a proper selection of the training dataset is clearly seen in Fig. 3 where our results are compared with machine learning extrapolations ISU-a [11] and ISU-b [16] which differ only by the range of $\hbar\Omega$ values included

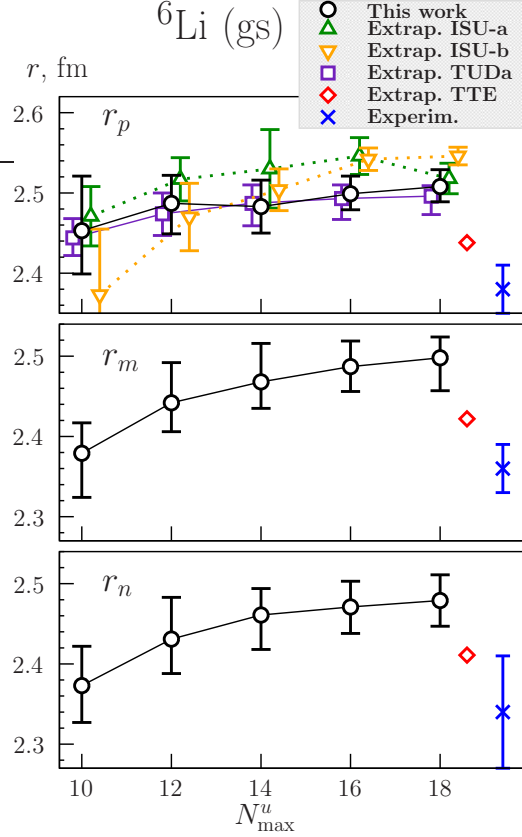


Figure 3: Extrapolation results (black circles) for rms point radii r_p , r_m and r_n in the ${}^6\text{Li}$ ground state with increasing training data sets including the NCSM results obtained with $N_{\text{max}} \leq N_{\text{max}}^u$. For comparison: blue oblique crosses present experimental values [31], green triangles, orange triangles and violet diamonds present respectively machine learning extrapolations ISU-a [11], ISU-b [16] and TUDa [16], and red diamonds present TTE extrapolations [32].

in the sets of the NCSM results for the training. The convergence of the ISU-b version is clearly worse and the final ISU-a and ISU-b results at $N_{\text{max}}^u = 18$ only slightly overlap if the uncertainties are taken into account. From our experience, it is better to exclude small $\hbar\Omega$ values in the training datasets for the radii extrapolations. Our predicted rms point-proton radius r_p is in agreement with the results of machine learning approaches ISU-a and TUDa.

As compared to the ground state, in the case of the first excited state ($3^+, 0$) of the ${}^6\text{Li}$ nucleus, the uncertainties of the extrapolated values of the rms point radii r_p , r_m , and r_n are significantly larger (see Table 2). However,

Nucleus (state)	rms radii	Cross point	This work	Experim.	Other
${}^6\text{He}(g.s.)$	r_p	1.86	1.93(2)	1.925(12)	1.871(6) TTE
	r_m	2.42	$2.50^{+0.03}_{-0.04}$	2.50(5)	2.430(6) TTE
	r_n	2.64	$2.77^{+0.02}_{-0.04}$	2.74(7)	2.663(3) TTE
${}^6\text{Li}(g.s.)$	r_p	2.44	2.51(2)	2.38(3)	2.411 TTE 2.518(19) ISU-a 2.546(11) ISU-b $2.496^{+0.013}_{-0.023}$ TUDa
	r_m	2.44	$2.50^{+0.03}_{-0.04}$	2.36(3)	2.422 TTE
	r_n	2.43	2.48(3)	2.34(7)	2.438 TTE
${}^6\text{Li}(3^+, 0)$	r_p	2.38	$2.45^{+0.04}_{-0.06}$	-	-
	r_m	2.26	2.42(9)	-	-
	r_n	2.30	$2.44^{+0.07}_{-0.09}$	-	-
${}^6\text{Li}(0^+, 1)$	r_p	2.48	$2.66^{+0.06}_{-0.09}$	-	-
	r_m	2.42	2.61(5)	-	-
	r_n	2.40	2.59(5)	-	-

Table 2: Extrapolated point-proton r_p , point-nucleon r_m , and point-neutron r_n radii (in fm) in the ${}^6\text{He}$ and ${}^6\text{Li}$ ground states and in the lowest excited states in ${}^6\text{Li}$ obtained using the largest training dataset ($N_{max}^u = 18$) in comparison with experimental data [31], TTE extrapolations from Ref. [32] for ${}^6\text{Li}$ and from Ref. [33] for ${}^6\text{He}$ and machine learning extrapolations ISU-a [11], ISU-b [16] and TUDa [16]. The symmetric uncertainties of the last presented digits are given in parentheses while asymmetric uncertainties are given in super and subscripts.

the overall convergence remains reasonably good. Similar to the ground state, the values of r_p , r_m , and r_n are close to each other. The central values of all these radii are slightly smaller the respective values in the ground state but overlap with them if the extrapolation uncertainties are taken into account.

The second excited state ($0^+, 1$) of ${}^6\text{Li}$ and the ground states ($0^+, 1$) of ${}^6\text{He}$ and ${}^6\text{Be}$ nuclei form an isospin triplet. Comparing the energies and rms radii of these states provides valuable insights into their structural similarities and differences. The convergence of the ${}^6\text{He}$ rms point radii with N_{max}^u is presented in Fig. 4.

Unlike the ($0^+, 1$) state in ${}^6\text{Li}$, the rms point-proton radius r_p of the

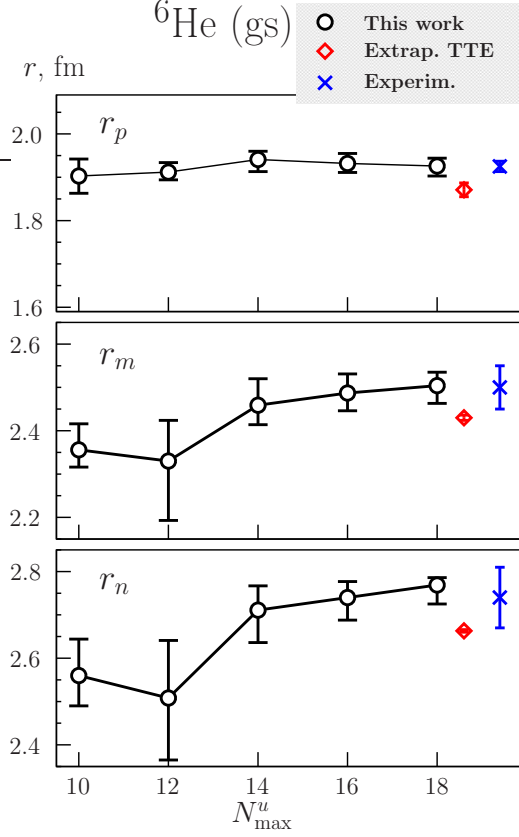


Figure 4: Extrapolation results (black circles) for rms point radii r_p , r_m and r_n in the ${}^6\text{He}$ ground state with increasing training data sets including the NCSM results obtained with $N_{\max} \leq N_{\max}^u$. For comparison: blue oblique crosses present experimental values [31] and red diamonds present TTE extrapolations [33].

${}^6\text{He}$ nucleus, as seen in Table 2, is much smaller than its point-neutron radius r_n revealing the two-neutron halo structure of this nucleus. The rms point-nucleon radius r_m lies between these two values satisfying with a good accuracy the well-known relation

$$Ar_m^2 = Zr_p^2 + Nr_n^2. \quad (1)$$

A comparison of predicted rms point radii with the experimental data and the results of the phenomenological $2D$ TTE extrapolation [32, 33] is presented in Table 2. Notably, our ${}^6\text{He}$ results agree with the experiment for radii while the predicted ${}^6\text{He}$ ground state energy (see Table 1) lies slightly below the experimental value.

4. Discussion

Using our modification [17, 18] of the machine learning method proposed in Ref. [11], we perform extrapolations to the infinitely large model space of the NCSM results for energies E and rms point-proton r_p , point-neutron r_n , and point-nucleon (matter) r_m radii of the ${}^6\text{He}$ nucleus in the ground state and in the three lowest states of the ${}^6\text{Li}$ nucleus. The NCSM calculations were performed using the Daejeon16 NN interaction in model spaces up to $N_{\text{max}} = 18$. The training datasets for the neural networks consist of the NCSM parameters N_{max} and $\hbar\Omega$ alongside with corresponding computed values of E (or r_p , r_n , or r_m).

The key innovation of our method is the training of an ensemble of artificial neural networks based on a preprocessing of training data, filtering trained networks according to rigorous selection criteria, and performing statistical post-processing of the accepted predictions. The extrapolation algorithm is implemented using Python with open-source machine learning libraries, including Keras [22], TensorFlow [23], and TensorFlow Addons [27].

The predictions for the ground state energies of ${}^6\text{Li}$ and ${}^6\text{He}$ exhibit a good convergence. By extrapolations utilizing the largest training dataset including the NCSM results in model spaces up to $N_{\text{max}}^u = 18$ we obtain $E({}^6\text{Li}) = -32.036 \pm 0.003$ MeV and $E({}^6\text{He}) = -29.429_{-0.005}^{+0.007}$ MeV. The prediction uncertainties are comparable to the numerical accuracy of NCSM calculations (1 keV) and do not exceed the uncertainties of the machine learning extrapolations ISU-a, ISU-b and TUDa. However, as it was shown in Refs. [17, 18], at all values of N_{max}^u , our extrapolation results lie systematically higher than those of ISU-a including the uncertainties. This suggests that different machine learning extrapolation approaches may lead to systematically different results. It is interesting that our prediction for the ${}^6\text{Li}$ ground state energy is consistent with the ISU-b prediction which uncertainty is, however, nearly an order of magnitude larger. Notably, due to the larger number of trained and selected neural networks in our study, the statistical reliability of our predictions is higher than those of ISU-a and ISU-b. The convergence trends of the TUDa approach for the energies is similar to ours but the final TUDa result suggests less binding of the ${}^6\text{Li}$ nucleus and does not overlap with ours accounting for the uncertainties.

The prediction uncertainty for rms point-proton, point-neutron and point-nucleon (matter) radii is slightly larger, approximately 1%, yet the overall convergence remains satisfactory. Our results for the radii of ${}^6\text{He}$ are in

excellent agreement with experimental data [31], while for ${}^6\text{Li}$, our predictions slightly exceed the experimental values. In general, our extrapolated rms radii are a bit larger than those obtained using a two-dimensional phenomenological exponential extrapolation TTE in the case of ${}^6\text{He}$ [33] and ${}^6\text{Li}$ [32] nuclei. The rms point-proton ${}^6\text{Li}$ radii predicted using the machine learning methods ISU-a and TUDa are close to ours while the ISU-b prediction lies above the results of all other extrapolations and the experiment. It is important to note the consistency of the predictions and nearly identical convergence trends (see Fig. 3) of our approach and that of the TUDa model for the rms point-proton radius in ${}^6\text{Li}$ contrary to the ISU-a and ISU-b convergence patterns.

Overall, our results indicate that machine learning offers a promising tool for addressing longstanding challenges in nuclear many-body theory. We anticipate that the proposed extrapolation method is rather general and can be applied to other nuclear observables, such as quadrupole moments, electromagnetic transition probabilities, etc.

5. Acknowledgements

This work was supported by the Ministry of Science and Higher Education of the Russian Federation (project No. FEME-2024-0005)

References

- [1] A. Boehnlein, et al., Machine learning in nuclear physics, *Rev. Mod. Phys.* 94 (2022) 031003. doi:10.1103/RevModPhys.94.031003.
- [2] R. Barrett, P. Navrátil, J. P. Vary, *Ab initio* no core shell model, *Prog. Part. Nucl. Phys.* 69 (2013) 131–181. doi:10.1016/j.ppnp.2012.10.003.
- [3] H. Zhan, A. Nogga, B. R. Barrett, J. P. Vary, P. Navrátil, Extrapolation method for the no-core shell model, *Phys. Rev. C* 69 (2004) 034302. doi:10.1103/PhysRevC.69.034302.
- [4] P. Maris, J. P. Vary, A. M. Shirokov, *Ab initio* no-core full configuration calculations of light nuclei, *Phys. Rev. C* 79 (2009) 014308. doi:10.1103/PhysRevC.79.014308.

- [5] S. A. Coon, M. I. Avetian, M. K. G. Kruse, U. van Kolck, P. Maris, J. P. Vary, Convergence properties of *ab initio* calculations of light nuclei in a harmonic oscillator basis, *Phys. Rev. C* 86 (2012) 054002. doi:10.1103/PhysRevC.86.054002.
- [6] P. Maris, J. P. Vary, *Ab initio* nuclear structure calculations of *p*-shell nuclei with JISP16, *Int. J. Mod. Phys. E* 22 (2013) 1330016. doi:10.1142/S0218301313300166.
- [7] S. N. More, A. Ekström, R. J. Furnstahl, G. Hagen, T. Papenbrock, Universal properties of infrared oscillator basis extrapolations, *Phys. Rev. C* 87 (2013) 044326. doi:10.1103/PhysRevC.87.044326.
- [8] M. K. G. Kruse, E. D. Jurgenson, P. Navrátil, B. R. Barrett, W. E. Ormand, Extrapolation uncertainties in the importance-truncated no-core shell model, *Phys. Rev. C* 87 (2013) 044301. doi:10.1103/PhysRevC.87.044301.
- [9] R. J. Furnstahl, S. N. More, T. Papenbrock, Systematic expansion for infrared oscillator basis extrapolations, *Phys. Rev. C* 89 (2014) 044301. doi:10.1103/PhysRevC.89.044301.
- [10] A. M. Shirokov, A. I. Mazur, V. A. Kulikov, On the convergence of oscillator basis calculations, *Phys. At. Nucl.* 84 (2) (2021) 131. doi:10.1134/S1063778821020149.
- [11] G. A. Negoita, J. P. Vary, G. R. Luecke, R. Glenn, P. Maris, A. M. Shirokov, I. J. Shin, Y. Kim, E. G. Ng, C. Yang, M. Lockner, G. M. Prabhu, Deep learning: Extrapolation tool for *ab initio* nuclear theory, *Phys. Rev. C* 99 (2019) 054308. doi:10.1103/PhysRevC.99.054308.
- [12] W. G. Jiang, G. Hagen, T. Papenbrock, Extrapolation of nuclear structure observables with artificial neural networks, *Phys. Rev. C* 100 (2019) 054326. doi:10.1103/PhysRevC.100.054326.
- [13] I. Vidaña, Machine learning light hypernuclei, *Nucl. Phys. A* 1032 (2023) 122625. doi:10.1016/j.nuclphysa.2023.122625.
- [14] M. Knöll, T. Wolfgruber, M. L. Agel, C. Wenz, R. Roth, Machine learning for the prediction of converged energies from *ab initio* nuclear structure calculations, *Phys. Lett. B* 839 (2023) 137781. doi:https://doi.org/10.1016/j.physletb.2023.137781.

- [15] T. Wolfgruber, M. Knöll, R. Roth, Precise neural network predictions of energies and radii from the no-core shell model, *Phys. Rev. C* 110 (2024) 014327. doi:10.1103/PhysRevC.110.014327.
- [16] M. Knöll, M. Lockner, P. Maris, R. J. McCarty, R. Roth, J. P. Vary, T. Wolfgruber, Benchmarking ANN extrapolations of the ground-state energies and radii of Li isotopes (2025). arXiv:2501.18252, doi:10.48550/arXiv.2501.18252.
- [17] A. I. Mazur, R. E. Sharypov, A. M. Shirokov, Machine learning in the problem of extrapolating variational calculations in nuclear physics, *Moscow Univ. Phys. Bull.* 79 (3) (2024) 318–329. doi:10.3103/S0027134924700395.
- [18] R. E. Sharypov, A. I. Mazur, A. M. Shirokov, Machine learning in the problem of no-core shell model result extrapolations, *Phys. At. Nucl.* 87 (Suppl. 2) (2024) S400–S408. doi:10.1134/S1063778824700868.
- [19] A. M. Shirokov, I. J. Shin, Y. Kim, M. Sosonkina, P. Maris, J. P. Vary, N3LO NN interaction adjusted to light nuclei in *ab initio* approach, *Phys. Lett. B* 761 (2016) 87–91. doi:10.1016/j.physletb.2016.08.006.
- [20] V. G. J. Stoks, R. A. M. Klomp, C. P. F. Terheggen, J. J. de Swart, Construction of high-quality nn potential models, *Phys. Rev. C* 49 (1994) 2950–2962. doi:10.1103/PhysRevC.49.2950.
- [21] X. Glorot, Y. Bengio, Understanding the difficulty of training deep feedforward neural networks, in: Y. W. Teh, M. Titterton (Eds.), *Proceedings of the Thirteenth International Conference on Artificial Intelligence and Statistics*, Vol. 9 of *Proceedings of Machine Learning Research*, PMLR, Chia Laguna Resort, Sardinia, Italy, 2010, pp. 249–256. URL <https://proceedings.mlr.press/v9/glorot10a.html>
- [22] F. Chollet, et al., Keras (2015). URL <https://keras.io>
- [23] M. Abadi, et al., TensorFlow: Large-scale machine learning on heterogeneous systems, software available from [tensorflow.org](https://www.tensorflow.org) (2015). URL <https://www.tensorflow.org/>

- [24] shadowcaramel, shadowcaramel/ncsmextrap: v0.1-alpha (Feb. 2025). doi:10.5281/zenodo.14928073.
- [25] D. P. Kingma, J. Ba, Adam: A method for stochastic optimization (2017). arXiv:1412.6980v9, doi:10.48550/arXiv.1412.6980.
- [26] L. N. Smith, Cyclical learning rates for training neural networks, in: 2017 IEEE winter conference on applications of computer vision (WACV), IEEE, 2017, pp. 464–472.
- [27] Tensorflow Addons (2024).
URL <https://github.com/tensorflow/addons>
- [28] A. Power, Y. Burda, H. Edwards, I. Babuschkin, V. Misra, Grokking: Generalization beyond overfitting on small algorithmic datasets (2022). doi:10.48550/arXiv.2201.02177.
- [29] R. R. Wilcoxon, Basic statistics: understanding conventional methods and modern insights, Oxford University Press, 2009. doi:10.1093/oso/9780195315103.001.0001.
- [30] D. Tilley, C. Cheves, J. Godwin, G. Hale, H. Hofmann, J. Kelley, C. Sheu, H. Weller, Energy levels of light nuclei $A = 5, 6, 7$, Nucl. Phys. A 708 (1) (2002) 3–163. doi:10.1016/S0375-9474(02)00597-3.
- [31] I. Tanihata, H. Savajols, R. Kanungo, Recent experimental progress in nuclear halo structure studies, Prog. Part. Nucl. Phys. 68 (2013) 215. doi:10.1016/j.pnpnp.2012.07.001.
- [32] D. M. Rodkin, Y. M. Tchuvil’sky, Sizes of the neutron–proton halo in nucleon-stable states of the ${}^6\text{Li}$ nucleus, JETP Lett. 118 (3) (2023) 153–159. doi:10.1134/S0021364023602130.
- [33] D. M. Rodkin, Y. M. Tchuvil’sky, Two-dimensional extrapolation procedure for an *ab initio* study of nuclear size parameters and the properties of the halo nucleus ${}^6\text{He}$, Phys. Rev. C 106 (2022) 034305. doi:10.1103/PhysRevC.106.034305.